2011-01-01

Optimal Control Applied to a Discrete Time Influenza Model

Paula Andrea Gonzalez Parra
University of Texas at El Paso, paulag817@gmail.com

OPTIMAL CONTROL APPLIED TO A DISCRETE TIME INFLUENZA MODEL

PAULA A. GONZALEZ PARRA

Program in Computational Science

APPROVED:

Leticia Velazquez, Chair, Ph.D.

Carlos Castillo-Chavez, Co-Chair Ph.D.

Miguel Argaez, Ph.D.

Martine Ceberio, Ph.D.

Sara Del Valle, Ph.D.

Benjamin C. Flores, Ph.D.
Acting Dean of the Graduate School

to my family and

to the memory

of my aunt Blanca Ines

she always was my support and motivation.

OPTIMAL CONTROL APPLIED TO A DISCRETE TIME INFLUENZA MODEL

by

PAULA A. GONZALEZ PARRA

THESIS

Presented to the Faculty of the Graduate School of

The University of Texas at El Paso

in Partial Fulfillment

of the Requirements

for the Degree of

MASTER OF SCIENCE

Program in Computational Science

THE UNIVERSITY OF TEXAS AT EL PASO

December 2011

Abstract

For the last decades, mathematical epidemiological models have been used to understand the dynamics of infectious diseases and guide public health policy. In particular, several continuous models have been considered to study influenza outbreaks and their controls policies. However, most epidemiological data is discrete; therefore, a discrete formulation is more convenient to compare collected data with the output of the model. We introduce a discrete time model in order to study optimal control strategies for influenza transmission.

In our model, we divide the population into four classes: susceptible, infectious, treated, and recovered individuals. In particular, we evaluate the potential effect of control measures, such as social distancing and antiviral treatment, on the dynamics of a single influenza outbreak. The objective is to reduce the total number of infected individuals at the end of the epidemic in a most economical way.

We solve the problem by using two different techniques. The first one is a discrete version of Pontryagin's maximum principle, which uses the forward-backward algorithm. In the second approach, we propose to solve the problem by using the primal-dual interior-point method that enforces physical conditions explicitly. We conclude that the primal-dual interior-point algorithm solves the problem more efficiently than the forward-backward algorithm, in terms of number of iterations and with a competitive value at the solution.

Finally, we include age structure in the model and analyze disease dynamics in different age classes. Our goal is to determine how treatment doses should be distributed and how social distancing should be implemented in each age group in order to reduce the final epidemic size.

Table of Contents

Page

Abstract iv

Table of Contents v

List of Tables vi

List of Figures vii

Chapter

1 Introduction 1

1.1 Epidemiological Model 2

1.2 Optimal Control Problem 3

2 Formulation 6

2.1 Pontryagin's Maximum Principle 6

2.1.1 Forward-Backward Method 7

2.2 Primal-Dual Interior-Point Method 9

2.2.1 Primal-Dual Interior-Point Method for The Optimal Control Problem 11

3 Numerical Results 14

3.1 Comparison Between Forward-Backward and Primal-Dual Interior-Point Method 14

3.2 Implication of Strategies 18

4 Age-Structured Model 23

4.1 Optimal Control Problem 27

5 Conclusions and Future Work 28

References 30

Curriculum Vitae 34

List of Tables

3.1 Definition of parameters and baseline values. 15
3.2 Comparison between Forward-Backward and Primal-Dual Interior-Point Method. 16
3.3 Comparison of strategies for low and moderate values of R_0 in reducing the final epidemic size. 20
3.4 Different weight constants in Strategies 1 and 2 22

List of Figures

1.1 Compartmental flow diagram for the SIR Model. 2

1.2 Compartmental flow diagram for the control SITR Model. 4

2.1 Geometrical interpretation of IPM in the case of linear programming. Each edge represents a linear constraint, the magenta line is the solution set. . . . 9

3.1 Strategy 1 (Social distancing): Figures A and B show the solution using FB and Figures C and D show the solution using IPM. Figures A and C are the optimal control solutions for each methodology, and Figures B and D illustrate the final epidemic size with and without control. The figures demonstrate the behavior is the same for both methods. 16

3.2 Strategy 2 (Only treatment): the solutions using FB algorithm are presented in Figures A and B, and the solutions using IPM are shown in Figures C and D. The optimal controls are shown in plots A and C, while the final epidemic size with and without control are shown in Figures B and D. The figures show the same behavior for both methods. 17

3.3 Strategy 3 (Social distancing and treatment): Figures A and B show the solutions using FB and Figures C and D illustrate the solution using IPM. Figures A and C show the optimal controls and Figures B and D show the final epidemic size with and without control. 17

3.4 For different values of R_0, we show the final epidemic size under each strategy. We observe that dual policies (strategy 3) provides the greatest reduction in the final epidemic size. Notice that when $R_0 \geq 1.4$, social distancing is better than treatment. 18

3.5 For $R_0 = 1.5$, the optimal control solution for each strategy is given in Figures A and B. The final epidemic size is reduced under the implementation of each strategy. For dual policies (treatment and social distancing), we get a reduction of 32%. The reduction for strategies 1 (social distancing) and 2 (treatment) are 28% and 25%, respectively. 19

3.6 For $R_0 = 2.5$, the optimal control solution for each strategy requires the maximum permitted values. The final epidemic size is reduced by 18% in strategy 3 (treatment and social distancing). For strategies 1 (social distancing) and 2 (treatment), the reductions are 22% and 7%, respectively. 20

3.7 For different values of the weight constant B_2, Figures A and B show the optimal control solution when strategy 1 is applied. Figure C shows the corresponding final epidemic size. When $B_2 = 0.1$, we get a significant reduction of 28%. 21

3.8 For strategy 2, Figure A shows the optimal control solution for different values of the weight constant B_3. Figure C shows the corresponding final epidemic size. When $B_3 = 0.01$, we get a reduction of 23%. 22

4.1 Figures A and B show the proportion of infected individuals and the final epidemic size in Group 1. If we apply control policies only in Group 1, we get a higher reduction in the final epidemic size. 26

4.2 Figures A and B show the proportion of infected individuals and the final epidemic size in Group 2. The number of infected individuals in Group 2 is reduced by the implementation of control policies in Group 1. We get a higher reduction in the final epidemic size when control policies are applied in Group 1. 26

Chapter 1

Introduction

In April of 2009, the World Health Organization (WHO) announced the emergence of a novel influenza A(H1N1) [13]. National and international public health agencies quickly took (often drastic) emergency measures to contain the spread of the virus; however, in June of 2009, the WHO declared novel influenza A (H1N1) a pandemic.

For the last decades, mathematical epidemiological models have been used to understand infectious disease dynamics and provide public health policy guidance. [3, 8, 19]. In particular, continuous time models have been used to study influenza outbreaks and the impact of different control policies [6, 14, 21, 31, 35]. Optimal control models have been used to evaluate the impact of control policies in many applications [7, 29, 32] including antiviral treatment and the isolation of infectious individuals [27, 28, 34]. Recently, more attention has been focused on discrete epidemiological models [1, 9, 10, 11, 37]. This is due to the fact that most epidemiological data is discrete; therefore, a discrete formulation is more convenient to compare collected data with the output of the model.

In this thesis, we introduce a discrete time epidemiological model and formulate an optimal control problem in order to evaluate the effect of social distancing and antiviral treatment as control measures. The optimal control problem is solved by using two different methodologies: a discrete version of the well-known Pontryagin's maximum principle and primal-dual interior-point method. To our knowledge, interior-point methods have not been previously used to solve control problems in epidemiology. The benefit of using this new approach is that it allows us to explicitly include upper bounds in the formulation.

1.1 Epidemiological Model

We formulate a discrete time Susceptible-Infectious-Recovered (SIR) model, where the total population (N) is divided into three classes: Susceptible (S), Infectious (I), and Recovered (R) individuals. Since we consider a single outbreak, births and deaths from natural causes are ignored ($N = S + I + R$). The subindex t denotes the number of individuals of each class at time t, and the range of $t \in [0, n]$, where n denotes the final time. The fraction of susceptible individuals at time t that get infected at time $t + 1$ is modeled by the function

$$G_t = \rho\gamma\frac{I_t}{N_t},$$

where ρ and γ are the susceptibility and infectiousness rate, respectively. The proportion of disease-induced deaths per generation is denoted by δ. It is assumed that infectious individuals *naturally* recover with probability σ_1 (per generation). In Figure 1.1, we present a diagram of the disease dynamics for the SIR model.

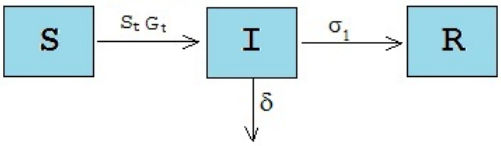

Figure 1.1: Compartmental flow diagram for the SIR Model.

The model (without control) is given by the following system of nonlinear difference equations:

$$\begin{aligned} S_{t+1} &= S_t(1 - G_t) \\ I_{t+1} &= S_t G_t + (1 - \sigma_1)(1 - \delta) I_t \\ R_{t+1} &= R_t + \sigma_1 (1 - \delta) I_t. \end{aligned} \tag{1.1}$$

We calculate the basic reproductive number R_0 by using the next generation operator approach described in [2]. In epidemiology, R_0 is defined as the number of secondary cases produced by a single infected individual in a population of susceptible individuals. For the

SIR Model (1.1) R_0 is given by

$$R_0 = \frac{\rho\gamma}{1-(1-\sigma_1)(1-\delta)}.$$

In the next section, we introduce a model that includes control policies such as social distancing and antiviral treatment. Our goal is to study the impact of different control policies in reducing disease spread.

1.2 Optimal Control Problem

We present an optimization formulation that is called "an optimal control problem." These problems were introduced in the 1950's, motivated especially by aerospace applications [18]. The main idea is to find an optimal control solution for a system, that is described by differential or difference equations. Pontriagyn, Boltyanskii, and Gamkrelidza found the necessary conditions for finding an optimal solution [18] of this problem, and these optimality conditions are well-known as the Pontryagin's Principle. Hence, in this subsection, we modify the system of difference equations (1.1) in order to introduce social distancing and antiviral treatment as control variables. Our goal is to reduce the number of infected individuals by using a minimal effort in social distancing and antiviral treatment.

We consider that the fraction of infected individuals who are treated each generation is modeled by the *antiviral treatment control* function labeled as τ_t. The *social distancing control* function, denoted by x_t, models the reduction in the number of contacts per unit of time. Figure 1.2 shows the disease dynamics of the control Susceptible-Infected-Treated-Recovered (SITR) model.

Since treated individuals are still infectious, the fraction of susceptible individuals at time t that remain susceptible at time $t+1$ is modeled by the function

$$G_t = \rho\gamma(1-x_t)\frac{I_t+\epsilon T_t}{N_t}, \tag{1.2}$$

where ϵ represents the effectiveness of the treatment ($0 < \epsilon \leq 1$). Then the control model is

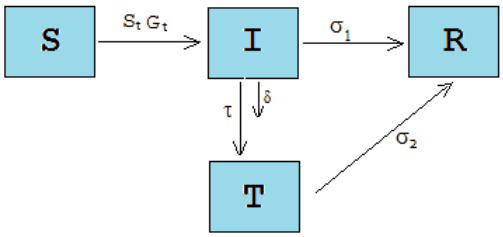

Figure 1.2: Compartmental flow diagram for the control SITR Model.

given by the following modified system of difference equations:

$$\begin{aligned} S_{t+1} &= S_t(1-G_t) \\ I_{t+1} &= S_t G_t + (1-\tau_t)(1-\sigma_1)(1-\delta) I_t \\ T_{t+1} &= (1-\sigma_2) T_t + \tau_t (1-\sigma_1)(1-\delta) I_t \\ R_{t+1} &= R_t + \sigma_1 (1-\delta) I_t + \sigma_2 T_t. \end{aligned} \tag{1.3}$$

Our goal is to minimize the number of infected individuals over a finite time interval $[0, n]$ by using the least amount of treatment and social distancing. Therefore, we pose the constrained optimal control model as

$$\text{minimize } \frac{1}{2} \sum_{t=0}^{n-1} \left(B_1 I_t^2 + B_2 x_t^2 + B_3 \tau_t^2 \right) \tag{1.4}$$

subject to Model 1.3,

$$0 \leq x_t \leq x_{\max},$$

$$0 \leq \tau_t \leq \tau_{\max},$$

where $x_{\max}$ and $\tau_{\max}$ are upper bounds that represent the maximum allowed values for each control per unit of time.

We evaluate the *relative* impact of each of the following control strategies applied to model (1.4):

Strategy 1: Only social distancing ($x_t \geq 0$, $\tau_t \equiv 0$),

Strategy 2: Only antiviral treatment ($\tau_t \geq 0$, $x_t \equiv 0$),

Strategy 3: Both social distancing and antiviral treatment ($x_t \geq 0$, $\tau_t \geq 0$).

The relative impact of each strategy is evaluated and compared from their effect on the final epidemic size, i.e., the number of infected individuals at the end of the epidemic, under single or dual policies. In our simulations we use perceived *relative* costs. Notice that each strategy will represent a different optimization problem. Each particular optimization problem is solved by using two different methodologies: the well-known discrete version of Pontryagin's maximum principle [22, 23, 29] and Primal-Dual Interior-Point Method [4, 5, 30, 17, 36]. The first method has been widely used to solve optimal control problems in epidemiology [16, 24, 27, 28]. The second technique has been applied successfully in different areas but to our knowledge, there is few evidences of applications on epidemiological problems. We present both methodologies in the next chapter.

Chapter 2

Formulation

In this chapter, we present two methodologies for solving the constrained optimal control problem (1.4): Pontryagin's maximum principle and primal-dual interior-point method.

2.1 Pontryagin's Maximum Principle

Pontryagin's maximum principle is a classical result of control theory that provides the necessary conditions for finding an optimal solution. Since our focus is to solve a discrete optimal control problem, we use a discrete version of Pontryagin's maximum principle [22, 23, 29].

We denote the control and state variables by $\mathbf{u} = (u_0, u_1, \ldots, u_{n-1})$ and $\mathbf{x} = (x_0, x_1, \ldots, x_n)$, respectively. The subindex represents the time step $t = 0, 1, \ldots, n$. The state equation for a given initial condition x_0, is given by the difference equation

$$x_{t+1} = g(x_t, u_t, t). \tag{2.1}$$

The objective functional is defined by

$$J(\mathbf{u}) = \Phi(x_n) + \sum_{t=0}^{n-1} f(x_t, u_t, t),$$

where f, g, and Φ are continuously differentiable functions; therefore, the constrained problem is

$$\begin{aligned} &\text{minimize} && J(\mathbf{u}) \\ &\text{subject to} && \text{Model (2.1).} \end{aligned}$$

We introduce the adjoint variable λ_t and define the Hamiltonian at time t for $t = 0, 1, \ldots, n-1$, as

$$H_t = f(x_t, u_t, t) + \lambda_{t+1} g(x_t, u_t, t).$$

The necessary conditions as described in [29] are given by

the adjoint equation

$$\lambda_t = \frac{\partial H_t}{\partial x_t}, \tag{2.2}$$

the transversality condition at the state solution x_n^*

$$\lambda_n = \Phi'(x_n^*),$$

and the optimality condition at the optimal solution u^*

$$\frac{\partial H_t}{\partial u_t} = 0.$$

These conditions are similar to the ones in the continuous case, but the only difference is that we do not have a negative sign in the adjoint equation (2.2). Usually in biological applications, the numerical solution is found by using the Forward-Backward algorithm [29]. This algorithm can be used for both the discrete and the continuous case.

2.1.1 Forward-Backward Method

In our particular optimization problem, we denote the control variables as $\mathbf{x} = (x_0, x_1, \ldots, x_{n-1})$ and $\boldsymbol{\tau} = (\tau_0, \tau_1, \ldots, \tau_{n-1})$ representing social distancing and treatment, respectively. Let $\mathbf{y}_t = (S_t, I_t, T_t, R_t)^T$ be the state variable with $t = 0, 1, \ldots, n$, and the objective functional

$$\mathcal{F}(\mathbf{x}, \boldsymbol{\tau}) = \frac{1}{2} \sum_{t=0}^{n-1} F(\mathbf{y}_t, x_t, \tau_t, t),$$

where

$$F(\mathbf{y}_t, x_t, \tau_t, t) = B_1 I_t^2 + B_2 x_t^2 + B_3 \tau_t^2. \tag{2.3}$$

The weight constants B_1 to B_3 are a measure of the *relative* cost of interventions over $[0, n]$. In particular, B_2 and B_3 denote the relative costs associated with the implementation of social distancing and antiviral treatment, respectively. The use of these notations and definitions lead to the problem of finding discrete control functions $\mathbf{x}$ and $\boldsymbol{\tau}$ such that

$$\begin{aligned} \underset{U}{\text{minimize}} \quad & \mathcal{F}(\mathbf{x}, \boldsymbol{\tau}) \\ \text{subject to} \quad & \text{Model (1.3)}, \end{aligned} \tag{2.4}$$

where $U = \{(x_t, \tau_t) : 0 \leq x_t \leq x_{\max}, 0 \leq \tau_t \leq \tau_{\max}, t = 0, 1, \ldots, n-1\}$. The Hamiltonian associated with Problem (2.4) is given by

$$H_t = F(\mathbf{y}_t, x_t, \tau_t, t) + \boldsymbol{\lambda}_{t+1}^T \mathbf{y}_{t+1},$$

for the control variables x_t, τ_t, the state and adjoint variables $\mathbf{y}_t, \boldsymbol{\lambda}_t \in \mathbb{R}^4$, respectively. The adjoint equations are

$$\lambda_t^i = \frac{\partial H_t}{\partial y_t^i}, \quad \text{with} \quad i = 1, 2, 3, 4, \tag{2.5}$$

where λ_t^i and y_t^i are the i-th component of $\boldsymbol{\lambda}_t$ and $\mathbf{y}_t$, respectively. Finally, the optimality conditions are $\frac{\partial H_t}{\partial x_t} = 0$ and $\frac{\partial H_t}{\partial \tau_t} = 0$.

The procedure to find optimal solutions is summarized in Algorithm 1.

Algorithm 1 Forward-Backward Algorithm

1: Initial values for $\mathbf{x}$, $\boldsymbol{\tau}$ and condition $\mathbf{y}_0$ are selected.

2: Solve the state equation (1.3) forward in time.

3: Solve the adjoint equation (2.5) backward in time; subject to the transversality conditions $\boldsymbol{\lambda}_n = 0$, where n is the final time.

4: Solve the optimality conditions $\frac{\partial H_t}{\partial x_t} = 0$ and $\frac{\partial H_t}{\partial \tau_t} = 0$.

5: Check convergence. That is, if $\frac{\|\mathbf{u} - \mathbf{u}_{old}\|}{\|\mathbf{u}\|} < 0.001$ for $\mathbf{u} \in \{\mathbf{x}, \boldsymbol{\tau}\}$, then stop. If $\frac{\|\mathbf{u} - \mathbf{u}_{old}\|}{\|\mathbf{u}\|} \geq 0.001$ go to Step 2.

2.2 Primal-Dual Interior-Point Method

Interior-Point Methods (IPM) were introduced by Karmarkar in 1984 [25] for solving linear programming problems and his seminal work has been extended for solving large scale non-linear programming problems (e.g., 2.4). Contrary to the simplex method, IPM find optimal solutions by crossing the interior of the feasible region. Figure 2.1 shows a geometrical interpretation of IPM in the case of linear programming when the solution set is an edge including the vertices.

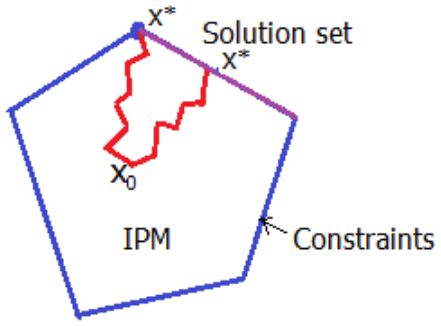

Figure 2.1: Geometrical interpretation of IPM in the case of linear programming. Each edge represents a linear constraint, the magenta line is the solution set.

Computationally, IPM are more efficient that the simplex method because they have polynomial complexity while simplex has exponential complexity. The simplex method finds solutions at the corner points only, while IPM finds solutions in the interior as well. The simplex method has shown to have exponential complexity, i.e., it may go through all the corners before finding a solution. Before introducing the interior-point methododology, we present some terminology and definitions.

A general nonlinear programming problem is given by

$$\begin{aligned} \text{minimize} \quad & f(x) \\ \text{subject to} \quad & h(x) = 0, \\ & x \geq 0, \end{aligned} \tag{2.6}$$

where $f : \mathbb{R}^n \to \mathbb{R}$ and $h : \mathbb{R}^n \to \mathbb{R}^m$. The Lagrangian function associated with Problem (2.6) is defined as

$$L(x, y, z) = f(x) + h(x)^T y - x^T z.$$

The Karush-Kuhn-Tucker (KKT) conditions are the necessary conditions for a solution of a nonlinear programming problem to be optimal. For Problem (2.6), the KKT conditions are given by

$$F(x, y, z) = \begin{bmatrix} \nabla_x L(x, y, z) \\ h(x) \\ XZe \end{bmatrix} = 0,$$

where $F : \mathbb{R}^{n+m+n} \to \mathbb{R}^{n+m+n}$, $\nabla_x L(x, y, z) = \nabla_x f + \nabla h(x)^T y - z$, $X = diag(x)$, $Z = diag(z)$, and $e = (1, \ldots, 1) \in \mathbb{R}^n$. Now we introduce the perturbed KKT conditions [4, 17] associated with Problem (2.6)

$$F_\mu(x, y, z) = \begin{bmatrix} \nabla_x L(x, y, z) \\ h(x) \\ XZe - \mu e \end{bmatrix} = 0, \tag{2.7}$$

where $F_\mu : \mathbb{R}^{n+m+n} \to \mathbb{R}^{n+m+n}$ and $\mu \geq 0$. Notice that the perturbation is made just in the last equation, known as the complementarity condition, in order to avoid "sticking to the boundary" before reaching a solution. The term "sticking to the boundary" refers to when an x_i or z_i becomes zero before reaching a solution, subsequently x_i^+ will be zero, i.e., if $x_i = 0$ and $z_i \neq 0$ then $\Delta x_i = 0$ and $x_i^+ = x_i + \Delta x_i = 0$, hence the algorithm will diverge. We use Newton's method to solve (2.7); therefore, the Jacobian associated with (2.7) is

$$F'(x, y, z) = \begin{bmatrix} \nabla_x^2 L & \nabla h(x)^T & I_{n\times n} \\ \nabla h(x) & 0_{m\times m} & 0_{m\times n} \\ Z & 0_{n\times m} & X \end{bmatrix},$$

the Newton system associated with (2.7) is given by

$$F'(x, y, z)\Delta s = -F_\mu(x, y, z), \tag{2.8}$$

where $\Delta s = [\Delta x, \Delta y, \Delta z]^T$.

2.2.1 Primal-Dual Interior-Point Method for The Optimal Control Problem

Now we can pose our Problem (1.4) as a nonlinear programming problem,

$$\begin{aligned} &\text{minimize} && f(y) \\ &\text{subject to} && E(y) = 0, \\ & && y \leq y_{\max}, \end{aligned} \tag{2.9}$$

where $\mathbf{y} = (S_1, I_1, T_1, x_0, \tau_0, \ldots, S_n, I_n, T_n, x_{n-1}, \tau_{n-1})$, n is the final time; in our simulations $n = 220$. The objective functional is given by $f : \mathbb{R}^{5n} \to \mathbb{R}$

$$f(y) = \frac{1}{2}\left(B_1|\tilde{I}|^2 + B_2|x|^2 + B_3|\tau|^2\right), \tag{2.10}$$

with $\tilde{I} = (I_0, I_1, \ldots, I_{n-1})$, $x = (x_0, x_1, \ldots, x_{n-1})$, and $\tau = (\tau_0, \tau_1, \ldots, \tau_{n-1})$.

From Model (1.3), we get the equality constraint $E : \mathbb{R}^{5n} \to \mathbb{R}^{3n}$,

$$E(y) = \begin{pmatrix} S_1 - S_0(1 - G_0) \\ I_1 - S_0 G_0 - (1 - \tau_0)(1 - \sigma_1) I_0 \\ T_1 - (1 - \sigma_2) T_0 - \tau_0 (1 - \sigma_1) I_0 \\ \vdots \\ S_n - S_{n-1}(1 - G_{n-1}) \\ I_n - S_{n-1} G_{n-1} - (1 - \tau_{n-1})(1 - \sigma_1) I_{n-1} \\ T_n - (1 - \sigma_2) T_{n-1} - \tau_{n-1} (1 - \sigma_1) I_{n-1} \end{pmatrix} = 0, \tag{2.11}$$

where G_i is given in (1.2). Here we assume $\delta \approx 0$, i.e., the mortality due to the disease is very small. Hence the total population N is almost constant, we could consider just S, I, and T because $R = N - S - I - T$. Finally, the inequality constraint can be written as $y_{\max} - y \geq 0$. This constraint represents the upper bounds for the controls u and τ, which are interpreted as the maximum daily rates.

Now we describe the primal-dual interior-point method uses to solve problem (2.9). We define the Lagrangian associated to (2.9) as

$$L(y, w, z) = f(y) + E(y)^T w - y^T z.$$

Therefore the perturbed KKT conditions are given by

$$F_\mu(y,w,z) = \begin{bmatrix} \nabla_y L(y,w,z) \\ E(y) \\ (Y_{\max} - Y)Z - \mu e \end{bmatrix} = 0, \tag{2.12}$$

where $F_\mu : \mathbb{R}^{5n+3n+5n} \to \mathbb{R}^{5n+3n+5n}$, $\nabla_y L(y,w,z) = \nabla_y f + \nabla E^T w - z$, $Y = diag(y)$, $Y_{\max} = diag(y_{\max})$, $Z = diag(z)$, and $e = (1,\ldots,1) \in \mathbb{R}^{5n}$. From (2.7) and (2.8), the Newton system associated with problem (2.9) is

$$\begin{bmatrix} \nabla^2 L & \nabla E^T & I_{5n\times 5n} \\ \nabla E & 0_{3n\times 3n} & 0_{3n\times 5n} \\ -Z & 0_{5n\times 3n} & (Y_{\max} - Y) \end{bmatrix}_{13n\times 13n} \begin{bmatrix} \Delta y \\ \Delta w \\ \Delta z \end{bmatrix} = - \begin{bmatrix} \nabla f + \nabla E^T W - z \\ E \\ (Y_{\max} - Y)Ze - \mu e \end{bmatrix}. \tag{2.13}$$

Notice that the Jacobian matrix of system (2.13) is non symmetric and highly indefinite. In order to work with a smaller system, we derive a reduced system associated with (2.13). We write explicitly the equations of (2.13).

$$\nabla^2 L\Delta y + \nabla E^T \Delta w + \Delta z = -\left(\nabla f + \nabla E^T W - z\right), \tag{2.14}$$

$$\nabla E \Delta y = -E, \tag{2.15}$$

$$-Z\Delta y + (Y_{\max} - Y)\Delta z = -\left((Y_{\max} - Y)Ze - \mu e\right), \tag{2.16}$$

and solving for Δz in (2.16),

$$\Delta z = (Y_{\max} - Y)^{-1} Z \Delta y - z + \mu (Y_{\max} - Y)^{-1} e. \tag{2.17}$$

By replacing (2.17) into (2.14) and (2.15) we get the reduced system

$$\begin{bmatrix} \nabla^2 L + \hat{Y} Z & \nabla E^T \\ \nabla E & 0_{3n\times 3n} \end{bmatrix}_{8n\times 8n} \begin{bmatrix} \Delta y \\ \Delta w \end{bmatrix} = \begin{bmatrix} -\nabla f - \nabla E^T W - \mu \hat{Y} e \\ -E \end{bmatrix}, \tag{2.18}$$

where $\hat{Y} = (Y_{\max} - Y)^{-1}$. Therefore, the reduced system of equations (2.18) has some advantages over (2.13) including that the Jacobian is symmetric and likely to be positive definite

as we add a positive definite matrix. Moreover, there is a considerable size reduction in the system being solved ($8n \times 8n$).

We use a *path-following* strategy [4, 5] to solve (2.13). For a $\mu > 0$ and working from the interior $(y_{\max} - y, z) > 0$, we apply a linesearch Newton's method [30] to the perturbed KKT conditions (2.12). An optimal solution is reached when the perturbation parameter μ goes to zero.

Now we present the primal-dual interior-point algorithm for the nonlinear programming problem (2.9).

Algorithm 2 Primal-Dual Interior-Point Algorithm

1: Consider an initial interior point $v_0 = (y_0, w_0, z_0)$, i.e., $(y_{\max} - y_0, z_0) > 0$, choose $\sigma \in (0, 1)$.

2: **for** $k = 0, 1, 2 \ldots$ until convergence **do**

3: Set the perturbed parameter $\mu_k = \sigma \frac{(y_{\max} - y_k)^T z_k}{5n}$.

4: Solve the reduced system (2.18) for $\Delta\nu = (\Delta y, \Delta w)$, and solve (2.17) for Δz.

5: Maintain $y_{\max} - y_0, z_0$ positive. Calculate $\tilde{\alpha_k}$ according to

$$\tilde{\alpha_k} = \min\left(\frac{-1}{\min(Z^{-1}\Delta z, -1)}, \frac{-1}{\min(-(Y_{\max} - Y)^{-1}\Delta y, -1)}\right)$$

6: Force a descent direction, For $i = 0, 1, 2, \ldots$, set $\alpha_{k+1} = \left(\frac{1}{2}\right)^i \tilde{\alpha_k}$ until

$$M(v_k + \alpha_{k+1}\Delta v) < M(v_k) + 10^{-4}\alpha_{k+1}\nabla M^T \Delta v$$

where $M = ||F_\mu||^2$, for F_μ as in (2.7).

7: Update $v_{k+1} = v_k + \alpha_{k+1}\Delta v$.

8: **If** $||F_\mu|| \leq \epsilon$, break,

9: **end for**

The numerical results of selected simulations generated by the implementation of both Pontryagin's maximum principle and primal-dual interior-point method are discussed in the next chapter.

Chapter 3

Numerical Results

The results of selected simulations generated by the implementation of the strategies described in Chapter 1 using Forward-Backward (FB) and Primal-Dual Interior-Point Method (IPM) are presented in this chapter. We use a moderate value for the basic reproductive number $R_0 = 1.5$ and a final time of 220 days. We solve Problem (1.4),

$$\text{minimize } \frac{1}{2}\sum_{t=0}^{n-1}\left(B_1 I_t^2 + B_2 x_t^2 + B_3 \tau_t^2\right)$$

$$\text{subject to Model 1.3,}$$

$$0 \leq x_t \leq x_{\max},$$

$$0 \leq \tau_t \leq \tau_{\max},$$

using the strategies presented in Chapter 1: only social distancing, only treatment, and dual policies (social distancing and treatment). Since we find that IPM solves the problem more efficiently than FB, in the second section we present some numerical solutions using only IPM. We study the impact of single and dual policies in the final epidemic size. The baseline parameter values are given in Table 3.1.

3.1 Comparison Between Forward-Backward and Primal-Dual Interior-Point Method

We show numerical simulations generated by solving problem (1.4) using the strategies presented in Chapter 1. For strategy 1 (only social distancing), the antiviral treatment control $\tau_t \equiv 0$ in the objective function F given in (2.3). For strategy 2 (only treatment), the social

Table 3.1: Definition of parameters and baseline values.

Parameter	Value	Definition
σ_1	$\frac{1}{7}$	Recovering probability without treatment
σ_2	$\frac{1}{5}$	Recovering probability with treatment
ϵ	0.8	Transmissibility of the treated class
δ	0.001	Mortality rate
ρ	0.5	Susceptibility rate
γ	$0.37 - 0.82$	Infectiousness rate
n	220	Final time (days)

distancing control $x_t \equiv 0$. Since we assume limited resources, the upper bounds for x_t and τ_t are $x_{\max} = 0.2$ and $\tau_{\max} = 0.2$ respectively; these values represent the maximum permitted value for each control policy daily. The weight constants B_1 to B_3, are a measure of the *relative* cost of interventions over $[0, n]$. In particular, B_2 and B_3, are the relative costs associated with the implementation of social distancing and antiviral treatment, respectively. In this particular case we consider $B_1 = 20$, $B_2 = 0.2$, and $B_3 = 0.1$. In this experimentation, the basic reproductive number is $R_0 = 1.5$. The numerical results are presented in Table 3.2. For each strategy, we tabulate the number of iterations and the value of the functional at the optimal solution (F^*) by using FB and IPM algorithms. We do not compare CPU time since both algorithms ran within least than two seconds.

In Table 3.2, we observe that for all strategies IPM requires fewer iterations to reach the solution with a competitive function value at the solution when compared to FB. Figures 3.1-3.3 show the level of intervention needed to control the epidemic and the final epidemic size with and without interventions for both methods for $R_0 = 1.5$.

Table 3.2: Comparison between Forward-Backward and Primal-Dual Interior-Point Method.

	Algorithm1: FB		Algorithm2: IPM	
Strategy	# of iterations	F^*	# of iterations	F^*
1 - Social Distancing	52	0.67997	11	0.68069
2 - Treatment	54	0.33014	10	0.33018
3 - Dual Policies	87	0.30423	23	0.30092

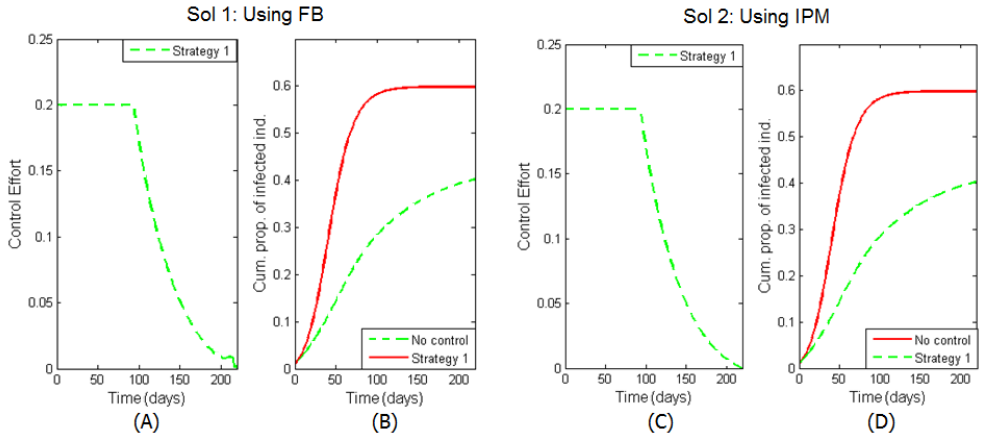

Figure 3.1: Strategy 1 (Social distancing): Figures A and B show the solution using FB and Figures C and D show the solution using IPM. Figures A and C are the optimal control solutions for each methodology, and Figures B and D illustrate the final epidemic size with and without control. The figures demonstrate the behavior is the same for both methods.

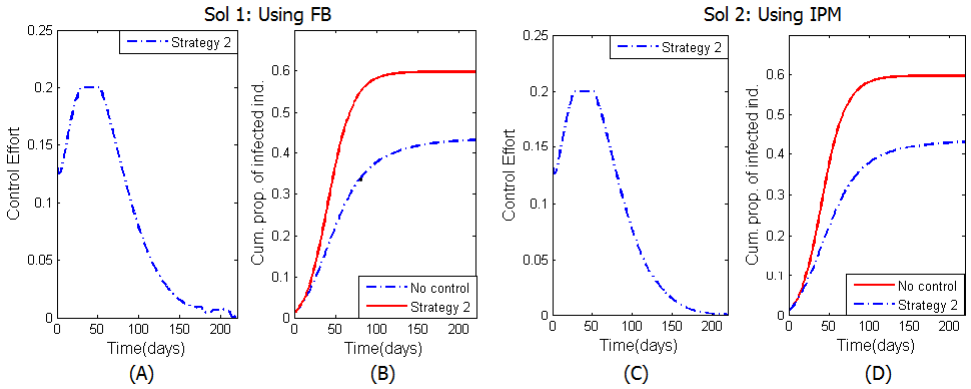

Figure 3.2: Strategy 2 (Only treatment): the solutions using FB algorithm are presented in Figures A and B, and the solutions using IPM are shown in Figures C and D. The optimal controls are shown in plots A and C, while the final epidemic size with and without control are shown in Figures B and D. The figures show the same behavior for both methods.

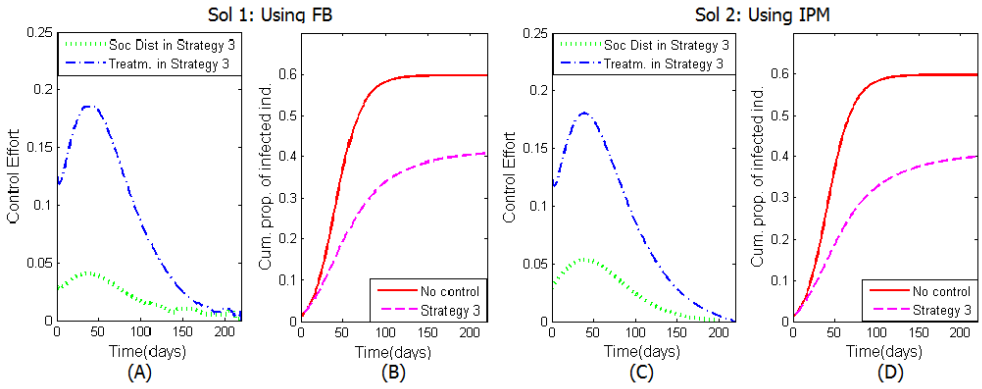

Figure 3.3: Strategy 3 (Social distancing and treatment): Figures A and B show the solutions using FB and Figures C and D illustrate the solution using IPM. Figures A and C show the optimal controls and Figures B and D show the final epidemic size with and without control.

3.2 Implication of Strategies

In this section, we present a comparison between strategies described in Chapter 1. The cumulative number of infected individuals for different values of R_0 in the absence of controls is compared against the presence of single or dual optimal controls. For single policies, a sensitivity analysis is carried out over the weight constants B_2 and B_3. In our simulations, we assume that the costs associated with social distancing are higher than those associated with treatment, i.e., $B_2 > B_3$. We compare the reduction in the final size as a result of the implementation of strategies 1 through 3. In these simulations, the values for the weight constants are $B_2 = 0.2$ and $B_3 = 0.1$. Results for low to high values of R_0 are presented in Figure 3.4.

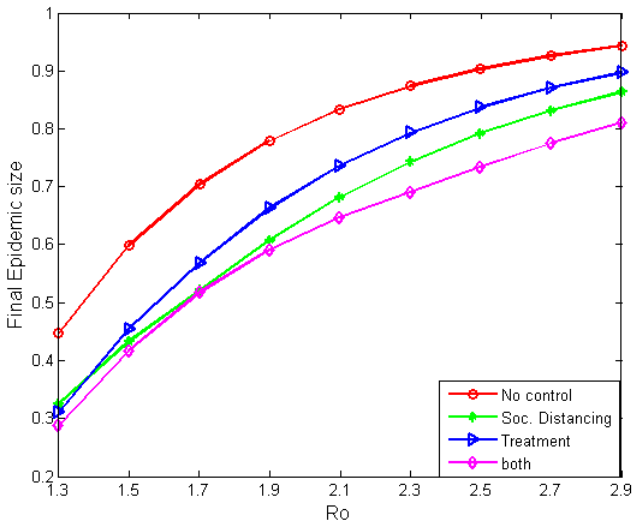

Figure 3.4: For different values of R_0, we show the final epidemic size under each strategy. We observe that dual policies (strategy 3) provides the greatest reduction in the final epidemic size. Notice that when $R_0 \geq 1.4$, social distancing is better than treatment.

Notice that the final epidemic size is reduced for all intervention strategies. The greatest reduction is in strategy 3, when we implement both social distancing and treatment. For single policies, Figure 3.4 shows that social distancing (strategy 1) is better than treatment

(strategy 2) for values of R_0 greater than 1.4.

Results under two different values of R_0, a low value ($R_0 = 1.5$) and a high value ($R_0 = 2.5$) are displayed in Figures 3.5 and 3.6, respectively. Figures 3.5(A,B) and 3.6(A,B) show the optimal control solution for social distancing and treatment, respectively, as a function of time for each strategy. In Figures 3.5(C) and 3.6(C), we compare the impact of each strategy on the cumulative proportion of infected individuals.

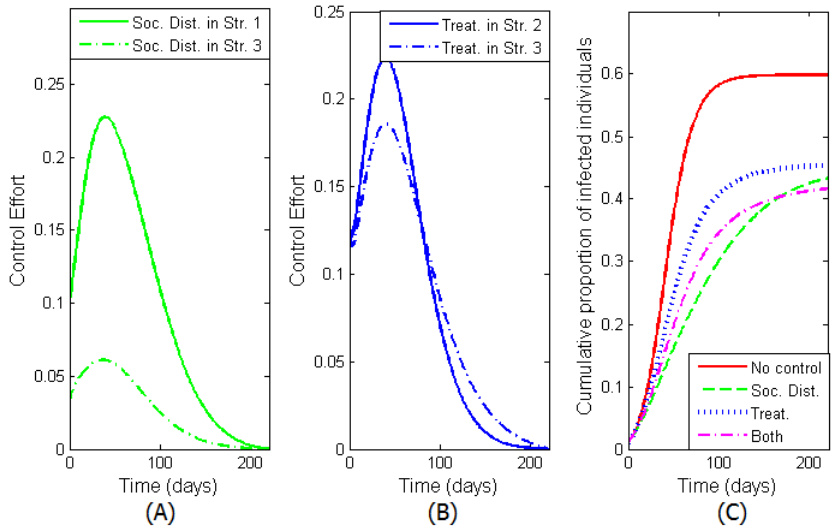

Figure 3.5: For $R_0 = 1.5$, the optimal control solution for each strategy is given in Figures A and B. The final epidemic size is reduced under the implementation of each strategy. For dual policies (treatment and social distancing), we get a reduction of 32%. The reduction for strategies 1 (social distancing) and 2 (treatment) are 28% and 25%, respectively.

For $R_0 = 1.5$, Figure 3.5(A,B) shows that the optimal control solution does not require the implementation of the maximum permitted values of social distancing and treatment, however, we get a substantial reduction in the final epidemic size. Figure 3.5(C) presents the best strategy, consisting of a 32% reduction (both social distancing and treatment).

The results for $R_0 = 2.5$ are given in Figure 3.6. In this case, the optimal control solution for all strategies requires the maximum allowed value. The reduction in the final epidemic size for each strategy is summarized in Table 3.3.

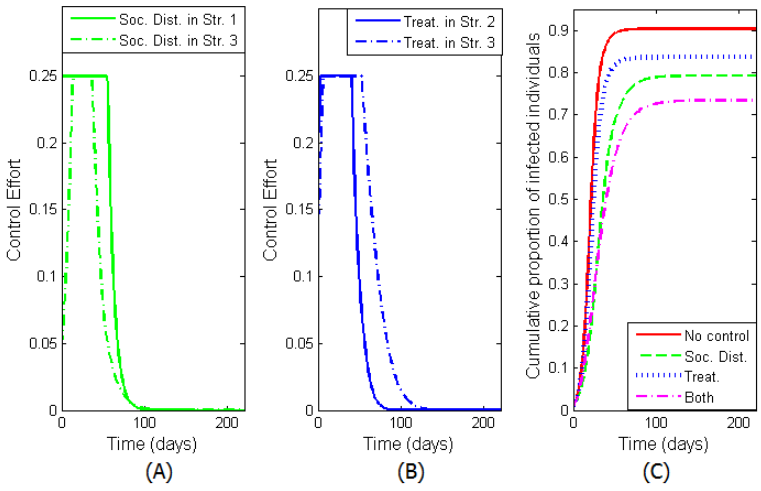

Figure 3.6: For $R_0 = 2.5$, the optimal control solution for each strategy requires the maximum permitted values. The final epidemic size is reduced by 18% in strategy 3 (treatment and social distancing). For strategies 1 (social distancing) and 2 (treatment), the reductions are 22% and 7%, respectively.

Table 3.3: Comparison of strategies for low and moderate values of R_0 in reducing the final epidemic size.

Strategy	Reduction for $R_0 = 1.5$	Reduction for $R_0 = 2.5$
1	28%	12%
2	25%	7%
3	32%	18%

Finally, we explore the quantitative impact of the weight constants in terms of the reduction in the cumulative infected individuals and final epidemic size. We study the impact of three different values for B_2 and B_3 on strategies 1 (social distancing) and 2 (antiviral treatment), respectively. We set $R_0 = 1.8$, $x_{\max} = 0.25$, and $\tau_{\max} = 0.25$.

Figures 3.7 and 3.8 show the optimal control solutions computed under strategies 1 and

2 as well as their impact on the cumulative proportion of infected individuals. Figure 3.7(A) shows that when the weight constant is small, $B_2 = 0.1$ (*relatively cheap*), the optimal control solution permits the maximum allowed value for social distancing within the first 110 days of the epidemic. This high value for the social distancing control yields the highest reduction of 27% in the final epidemic size (Figure 3.7(C)). When the weight constant $B_2 = 0.2$ (*moderate cost*), the reduction in the final epidemic size is 24%. However, if the weight constant is increased to $B_2 = 1$ (*relatively expensive*), the reduction in the final epidemic size decreases by 13%. Figure 3.7(B) shows the reduction in the peak of the epidemic as the value of the weight constant B_2 decreases. When Strategy 2 is applied, similar results are obtained. As the weight constant B_3 increases, reductions in the final epidemic size are observed. For example, when $B_3 = 0.01$, the reduction in the final epidemic size is 23% but when $B_3 = 1$ the reduction is only 10%. These results are summarized in Table 3.4.

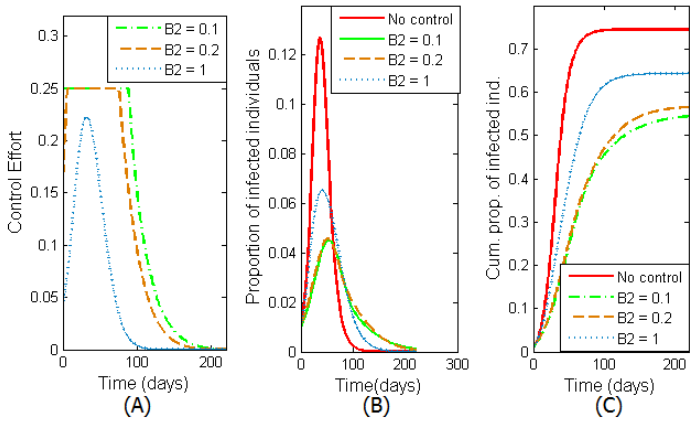

Figure 3.7: For different values of the weight constant B_2, Figures A and B show the optimal control solution when strategy 1 is applied. Figure C shows the corresponding final epidemic size. When $B_2 = 0.1$, we get a significant reduction of 28%.

In the next Chapter, we introduce an age structured model. The main idea for this model is to consider some individuals' demographic characteristics and behavior. We introduce

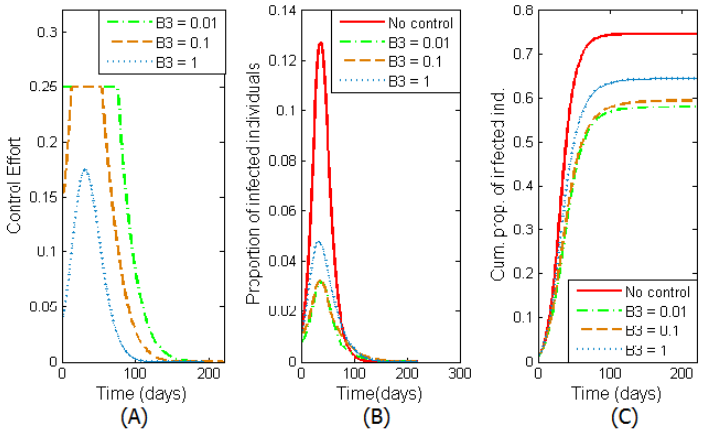

Figure 3.8: For strategy 2, Figure A shows the optimal control solution for different values of the weight constant B_3. Figure C shows the corresponding final epidemic size. When $B_3 = 0.01$, we get a reduction of 23%.

Table 3.4: Different weight constants in Strategies 1 and 2

Strategy 1		Strategy 2	
B2	Final epidemic size reduction	B3	Final epidemic size reduction
0.1	27%	0.1	23%
0.2	24%	0.2	21%
1	13%	1	10%

an optimal control problem associated with this age structured model, and our goal is to determine how control policies should be applied in each group in order to reduce the number of infected individuals.

Chapter 4

Age-Structured Model

In this chapter, we want to extend Model (1.1) presented in Chapter 1 by considering that the total population is divided into m subgroups. This division is based on how individuals mix with others; in this sense, groups can be defined according to age, economic status, individuals' behavior, etc. We assume that people mix homogeneously within each age group but they mix heterogeneously among other age groups; this is know as proportionate mixing. Epidemiological models with age structure have been considered in [12, 15, 20, 33]; the main motivation for this kind of models is that disease dynamics such as measles and influenza is strongly correlated with age [12]. We now introduce the age-structured model.

Let $N_i(t)$ be the number of individuals in the group i at time t, C_i the average contact rate of individuals in group i, and q_{ij} the probability that somebody from group i has contact with somebody from group j given that it has contact with somebody. We assume that all groups are connected ($q_{ij} > 0$) and we consider proportional mixing [12], hence we have

$$q_{ij} = q_j = \frac{C_j N_j}{\sum_{k=1}^{m} C_k N_k}. \tag{4.1}$$

In order to generalize the SIR model (1.3), let $S_i(t)$, $I_i(t)$, and $R_i(t)$ denote the number of susceptible, infectious, and recovered individuals in the ith group, $i = 1, ..., m$. Since we consider a single outbreak, age does not change during the epidemic; therefore people remain in the same group. We assume that infectious individuals from group i naturally recover with probability σ_i. The proportion of disease-induced deaths per generation in group i is denoted by δ_i. The fraction of susceptible individuals on group i at time t that get infected

at time $t+1$ is modeled by the function

$$G_i(t) = \rho_i \sum_{j=1}^{m} \left(q_j \gamma_j \left(\frac{I_j(t)}{N_j(t)} \right) \right), \tag{4.2}$$

where ρ_i and γ_i are the susceptibility and infectiousness rates from individuals in group i, respectively. The model is given by the system of difference equations

$$\begin{aligned} S_i(t+1) &= S_i(t)(1 - G_i(t)) \\ I_i(t+1) &= S_i(t)G_i(t) + (1-\sigma_i)\,(1-\delta_i)I_i(t) \\ R_i(t+1) &= R_i(t) + \sigma_i\,(1-\delta_i)\,I_i(t). \end{aligned} \tag{4.3}$$

The basic reproductive number is calculated by using the next generation operator [2], it is given by

$$R_0 = \sum_{j=1}^{m} \left(\frac{1}{1-(1-\sigma_j)(1-\delta_j)} \gamma_j \rho_j \frac{C_j N_j}{\sum_{k=1}^{m} C_k N_k} \right).$$

Notice that there is a contribution from each group: it highlights that new infections can be generated from infected individuals on any group.

The next step is to include treatment and social distancing as control policies in Model (4.3), in a similar way that we included it in the single group model (1.1) in Chapter 1.

We consider that the fraction of infected individuals in group i who get treatment each generation is modeled by $\tau_i(t)$. The *social distancing control* function, $x_i(t)$, models the reduction in the number of contacts per unit of time from individuals in group i. We assume that individuals (from any group) who get treatment recover with probability σ. Since treated individuals are still infectious, the function G_i given in (4.2) is modified as

$$G_i = \rho_i \sum_{j=1}^{m} \left(q_j \gamma_j (1 - x_j(t)) \left(\frac{I_j(t) + \epsilon_j T_j(t)}{N_j} \right) \right), \tag{4.4}$$

where ϵ_j represents the transmissibility for treated individuals on group j, with $0 < \epsilon_j \leq 1$.

The model with control is given by the following system of difference equations:

$$\begin{aligned} S_i(t+1) &= S_i(t)(1-G_i(t)) \\ I_i(t+1) &= S_i(t)G_i(t) + (1-\tau_i(t))\,(1-\sigma_i)\,(1-\delta_i)I_i(t) \\ T_i(t+1) &= (1-\sigma)\,T_i(t) + \tau_i(t)\,(1-\sigma_i)\,(1-\delta_i)I_i(t) \\ R_i(t+1) &= R_i(t) + \sigma_i\,(1-\delta_i)\,I_i(t) + \sigma T_i(t). \end{aligned} \tag{4.5}$$

Before introducing the optimal control problem associated with the age-structured model (4.5), let us present some numerical results. Consider two groups: people socially active are in Group 1 and less active individuals are in Group 2. If we apply constant control in only one group, we could consider two scenarios. In the first one, we only apply control in Group 1, $x_1(t) = 0.1$, $\tau_1(t) = 0.1$, $x_2(t) = 0$, and $\tau_2(t) = 0$, $t = 0, 1, \ldots, 250$; in the second one, we only apply control in Group 2, therefore $x_2(t) = 0.1$, $\tau_2(t) = 0.1$, $x_1(t) = 0$, and $\tau_1(t) = 0$ for $t = 0, 1, \ldots, 250$.

Figures 4.1 and 4.2 show the behavior of the proportion of infected individuals and the final epidemic size in Group 1 and 2 respectively. Notice that the number of infected individuals in one group is reduced by the implementation of control policies in the other group. However since Group 1 is more active, we get a higher reduction in the final epidemic size when control policies are applied in this group.

For this simple example, we just use constant values for the control function; however our future work is to estimate how control policies should be applied in order to minimize the number of infected individuals. In addition we need to consider some restrictions related with resources availability. Therefore we formulate an optimal control problem which will be solved by using primal-dual interior-point method.

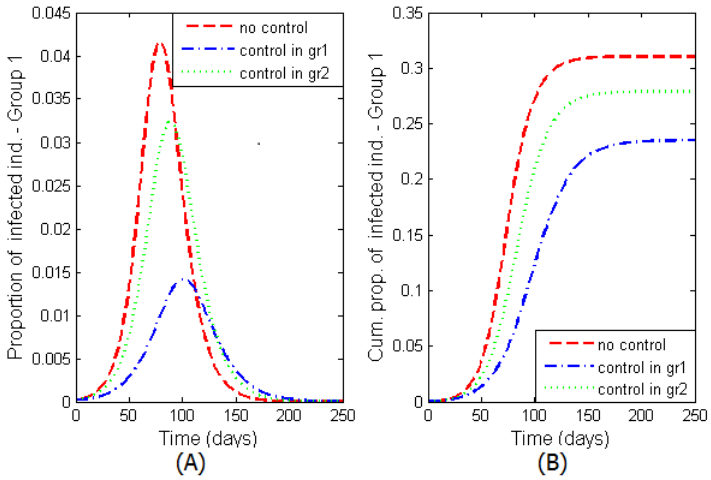

Figure 4.1: Figures A and B show the proportion of infected individuals and the final epidemic size in Group 1. If we apply control policies only in Group 1, we get a higher reduction in the final epidemic size.

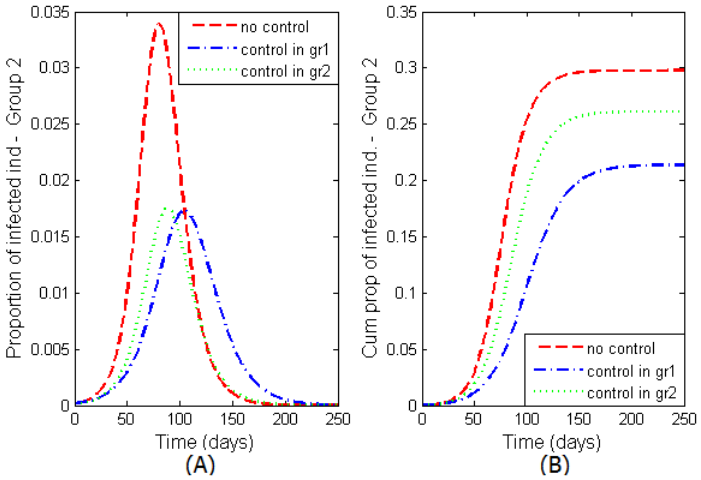

Figure 4.2: Figures A and B show the proportion of infected individuals and the final epidemic size in Group 2. The number of infected individuals in Group 2 is reduced by the implementation of control policies in Group 1. We get a higher reduction in the final epidemic size when control policies are applied in Group 1.

4.1 Optimal Control Problem

Our goal is to minimize the number of infected individuals over a finite interval $[0, n]$, by using a minimal effort on treatment and social distancing. Following the ideas in Chapter 1, we generalize the problem given in (1.4), therefore the optimal control problem associated with the age-structured model can be written as:

$$\begin{aligned} &\text{minimize } \frac{1}{2}\sum_{i=1}^{m}\left(\sum_{t=0}^{n-1}\left(B_1^i I_i(t)^2 + B_2^i x_i(t)^2 + B_3^i \tau_i(t)^2\right)\right) \\ &\text{subject to Model (4.5)}, \end{aligned} \tag{4.6}$$

where n and m denote the final time and the number of groups, respectively. As future work, we want to consider two scenarios: unlimited and limited doses of treatment. The first scenario is the problem given in (4.6). For the second one, we need to include the isoperimetric-constraint [28, 29]

$$\sum_{i=1}^{m}\left(\sum_{t=0}^{n-1}\left(\tau_i(t) I_i(t)\right)\right) = K, \tag{4.7}$$

where K represents the available number of treatment doses. A similar problem has been solved in [28] by considering limited vaccine in a continuous time influenza model. The problem was solved by using the Forward-Backward method; we will solve it by using primal-dual interior-point method. The authors remark that by including the isoperimetric-constraint, convergence issues have to be addressed. We claim that primal-dual interior-point method allows to include the new constraint more efficiently. Our goal is to determine how social distancing should be applied and how many doses should be distributed in each group in order to reduce the final epidemic size. In addition, we will include more classes in the model, for example, asymptomatic individuals or different levels of infectiousness. A discrete optimal control problem for influenza including asymptomatic individuals is presented in [26].

Chapter 5

Conclusions and Future Work

A discrete model is formulated in order to study single epidemic outbreaks in the context of influenza. An optimal control problem is formulated in order to minimize the number of infected individuals by using a minimal effort in treatment and social distancing. We compare three different strategies: only social distancing, only treatment, and both policies together.

The problem is solved by using two techniques: Forward-Backward algorithm and Primal Dual Interior-Point Method. The first one is well-known in many applications including epidemiological problems. The second one has been applied successfully in different areas but, as far as we know there is few applications on epidemiological problems. Our numerical results show that Primal Dual Interior-Point Method reaches the solution with fewer number of iterations and with a competitive function value at the solution when compared to Forward-Backward algorithm.

We found that the use of single and dual strategies (social distancing and antiviral treatment) results in reductions in the cumulative number of infected individuals. We have seen that dual strategies are more efficient at reducing the final epidemic size than single policies. Our results show that under the implementation of a single policy, the social distancing strategy (Strategy 1) is more effective than the antiviral treatment strategy (Strategy 2) when $R_0 > 1.4$.

An age-structured model is formulated under the assumption that people mix more with individuals in the same group and groups are mixing randomly. We formulate an optimal control problem (4.6) in order to study how control policies should be implemented in each group in order to reduce the number of infected individuals. Because of the introduction of

groups into the model, the problem becomes computationally more expensive; we will solve it by using primal-dual interior-point method.

As additional future work, we will include more classes in the model, such as asymptomatic individuals. We also want to consider the case of limited resources by including an isoperimetric-constraint (4.7). A continuous influenza model with limited supplies was studied in [28]. The authors remark that by including this constraint, convergence issues have to be addressed. We claim that primal-dual interior-point method allows to include the new constraint more efficiently. Furthermore, our goal is to consider a more realistic scenario, hence a parameter estimation in the model will be done by using real data.

References

[1] L.J. Allen and A.M. Burgin, "Comparison of deterministic and stochastic SIS and SIR models in discrete time," *Math. Biosci.*, 2000, Vol. 163, pp. 1–33.

[2] L.J. Allen and P. van den Driessche, "The basic reproductive number in some discrete time epidemic models," *Journal of difference equations and applications*, 2008, Vol. 14, No. 10-11, pp. 1127–1147.

[3] R.M. Anderson and R.M. May, *Infectious Diseases of Humans: Dynamics and Control*, Oxford University Press, Oxford, UK, 1992.

[4] M. Argaez, and R. Tapia, "On the Global Convergence of a Modified Augmented Lagrangian Interior-Point Newton Method for nonlinear programming." *Journal of Optimization Theory and Applications*, 2002, Vol. 114, pp. 1–25.

[5] M. Argaez, R. Tapia, and L. Velazquez. Numerical comparisons of path-following strategies for a primal-dual interior-point method for nonlinear programming. *Journal of Optimization Theory and Applications*, 2002, Vol. 114, No. 2.

[6] J. Arino, F. Brauer, P. van den Driessche, J. Watmough, and J. Wu, "A model for influenza with vaccination and antiviral treatment," *J. Theor. Biol.*, 2003, Vol. 253, pp. 118–130.

[7] H. Behncke, "Optimal control of deterministic epidemics," *Opt. Control Appl. Meth.*, 2000, Vol. 21, pp. 269–285.

[8] F. Brauer and C. Castillo-Chavez, *Mathematical Models in Population Biology and Epidemiology*, Springer-Verlag, 2001.

[9] F. Brauer, Z. Feng, and C. Castillo-Chavez, "Discrete epidemic models," *Math. Biosc. & Eng.*, 2010, Vol.7, pp. 1–15.

[10] C. Castillo-Chavez and A-A. Yakubu, "Discrete-time S-I-S models with complex dynamics," *Nonlinear Analysis*, 2001, Vol.47, pp. 4753–4762.

[11] C. Castillo-Chavez and A-A. Yakubu, "Discrete-time S-I-S models with simple and complex population dynamics," *Mathematical Approaches for Emerging and Reemerging Infectious Diseases*, (eds., C. Castillo-Chavez, et al.), Springer-Verlag, IMA, 2001, Vol. 125, pp. 153–163.

[12] C. Castillo-Chavez, H.W Hethcote, "Epidemiological models with age structure, proportionate mixing, and cross inmunity ." *Journal of mathematical biology*, 1989, Vol 27, pp. 233–258.

[13] M. Chan, "World now at the start of 2009 influenza pandemic", `http://who.int/mediacentre/news/statements/2009/h1n1\_pandemic\_phase6\_20090611/en/index.html`, 11 Jun. 2009.

[14] G. Chowell, C.E. Ammon, N.W. Hengartner, and J.M. Hyman, "Transmission dynamics of the great influenza pandemic of 1918 in Geneva, Switzerland: Assessing the effects of hypothetical interventions," *J. Theor. Biol.*, 2006, Vol. 241, pp. 193–204.

[15] S.Y Del Valle, J.M Hyman, H.W Hethcote, and S.G. Eubank. "Mixing patterns between age groups in social networks." *Social Networks*, 2007. Vol.29, pp. 539-554.

[16] W. Ding, L. Gross, K. Langston, S. Lenhart, and L. Real, "Rabies in racoons: optimal control for a discrete time model on a spatial grid", *J. Biol. Dynamics*, 2007, Vol. 1, pp. 307–393.

[17] A.S. El-Bakry, R.A. Tapia, T. Tsuchiya, and Y. Zhang. "On the Formulation and Theory of the Primal-Dual Newton Interior-Point Method for Nonlinear Programming," *Journal of Optimization Theory and Applications*. 1996. Vol. 89, No. 3, pp. 507–541.

[18] W.H. Fleming and R.W. Rishel. *Deterministic and Stochastic Optimal Control*, Springer Verlag. 1975.

[19] H.W. Hethcote, "The mathematics of infectious diseases," *SIAM Rev*, 2000, Vol. 42, pp. 599–653.

[20] H.W. Hethcote. "An Age-Structured Model for Pertusis Transmission." *Mathematical Biosciences*. 1997. Vol. 145, pp. 89–136.

[21] M.A. Herrera-Valdez, M. Cruz-Aponte and C. Castillo-Chavez, "Multiple outbreaks for the same pandemic: Local transportation and social distancing explain the different "waves" of A-H1N1pdm cases observed in Mxico during 2009," *Math. Biosc. & Eng.*, 2011, Vol. 8, pp. 21–48.

[22] R. Hilschera and V. Zeidanb, "Discrete optimal control: The accessory problem and necessary optimality conditions," *Journal of Mathematical Analysis and Applications*, 2000, Vol. 243, pp. 429–452.

[23] C. Hwang and L. Fan, "A Discrete version of Pontryagin's maximum principle," *Operations Research*, 1967, Vol. 15, pp. 139–146.

[24] E. Jung, S. Lenhart, V. Protopopescu, and C.F. Babbs, "Optimal control theory applied to a difference equation model for cardiopulmonary resuscitation," *Mathematical Models and methods in Applied Sciences*, 2005, Vol. 15, pp. 1519–1531.

[25] N. Karmarkar, "A New Polynomial Time Algorithm for Linear Programming," *Combinatorica*, 1984, Vol. 4, pp. 373–395.

[26] P. González-Parra, S. Lee, L. Velazquez, and C. Castillo-Chavez, "A note on the use of optimal control on a discrete time model of influenza dynamics." *Math. Biosc. & Eng.*, 2011, Vol. 8, No 8, pp. 183–197.

[27] S. Lee, G. Chowell, and C. Castillo-Chavez, "Optimal control for pandemic influenza: the role of limited antiviral treatment and isolation," *J.Theor. Biol.*, 2010, Vol. 265, pp. 136–150.

[28] S. Lee, R. Morales, and C. Castillo-Chavez, "A note on the use of influenza vaccination strategies when supply is limited," *Math. Biosc. & Eng.*, 2011, Vol. 8, pp. 171–182.

[29] S. Lenhart and J. Workman, *Optimal Control Applied to Biological Models*, Chapman & Hall, CRC Mathematical and Computational Biology series, 2007.

[30] J. Nocedal and S.J. Wright, *Numerical Optimization*, 2nd Edition. Springer Verlag. 2006.

[31] M. Nuno, G. Chowell, X. Wang, and C. Castillo-Chavez, "On the role of cross-immunity and vaccines on the survival of less fit flu-strains", *Theor. Pop. Biol.*, Elsevier, 2007, Vol.71, pp. 20–29.

[32] L.S. Pontryagin, V. Boltyanskii, R. Gamkrelidze, and E. Mishchenko, *The Mathematical Theory of Optimal Processes*, Wiley, New Jersey, 1962.

[33] C. Castillo-Chavez, H.W. Hethcote, "Epidemiological models with age structure, proportionate mixing, and cross inmunity ." *Journal of mathematical biology*, 1989, Vol. 27, pp. 233–258.

[34] J.M. Tchuenche, S.A. Kamis, F.B. Agusto, and S.C. Mpesche, "Optimal control and sensitivity analysis of an influenza model with treatment and vaccination," *Acta Biotheoretica*, Springer, 2010.

[35] S.M. Tracht, S. Del Valle, and J. Hyman, "Mathematical modeling of the effectiveness of facemasks in reducing the spread of novel influenza A (H1N1)" *PLoS ONE*, 2010, www.plosone.org, Vol.5.

[36] S. Wright, "Primal-Dual Interior-Point Methods." *Siam.* 2006.

[37] Y. Zhou, Z. Ma and F. Brauer, "A discrete epidemic model for SARS transmission and control in China," *Math. and Computer Modelling*, 2004, Vol.40, pp. 1491–1506.

Curriculum Vitae

Paula Andrea Gonzalez Parra was born on August 17, 1975 in Cali-Colombia. The first daughter of Luis Arturo Gonzalez and Maria Isabel Parra, she graduated from Universidad del Valle, Cali, in December of 1996 with a major in mathematics. She got her master in Mathematics in the same university on December of 2002. She was a teaching assistant and full time lecturer at the Mathematical Science Department in Universidad del Valle from 1996 to 2004. She worked as a full time lecturer at the militar school Marco Fidel Suarez in Cali. In 1998 she started working as a lecturer at the Universidad Autonoma de Occidente. In 2005 she got a full time position at this university. Paula was part of the organizing committee at the international conference APPOPT in San Andres, island, Colombia; where she met her doctoral advisor Leticia Velazquez. In the spring of 2009, Paula entered the Graduate School of The University of Texas at El Paso. She is a PhD student at the program in Computational Science and she has been working as a Research Assistant. She had the opportunity to met Dr Carlos Castillo-Chavez, her dissertation co-chair, and she has attended the Mathematical and Theoretical Biology Institute MTBI in 2000, 2009, 2010, and 2011 under the supervision of Dr Castillo-Chavez. Research publications for her previous work include: A note on the use of optimal control on a discrete time model of influenza dynamics. Mathematical Biosciences and Engineering, 2011; Optimal control applied to a discrete influenza model, Conference Proceedings Book of the XXXVI International Operation Research Applied to Health Services, 2010.

Permanent address: 200 N Festival Dr, Apt 1902
El Paso, Texas 79912
email: paulag817@gmail.com